Self-compression of laser pulses induced by asymmetric self-phase modulation aided by backward Raman scattering in periodic density-modulated plasma

Jiajun Li,[1,2] Hanchen Xue,[1,2] Zhaohua Wang,[1,2,3,*] Xianzhi Wang,[1,3] Jiawen Li,[1,2,3] Yingfeng Li,[1,2,3] Guodong Zhao,[1,2] and Zhiyi Wei[1,2,3,†]

[1]*Beijing National Laboratory for Condensed Matter Physics, Institute of Physics, Chinese Academy of Sciences, Beijing 100190, China*
[2]*University of Chinese Academy of Sciences, Beijing 100049, China*
[3]*Songshan Lake Materials Laboratory, Dongguan 523808, China*

(Received 4 March 2024; revised 7 May 2024; accepted 31 May 2024; published 13 June 2024)

Here a mechanism for self-compression of laser pulses is presented, based on period density-modulated plasma. In this setup, two pump beams intersect at a small angle within the plasma. This interaction is facilitated by the ponderomotive ion mechanism, which causes a modulation in the density of plasma with long wavelengths and low amplitude. This modulation enhances the backward Raman scattering of the probe pulse. The trailing edge of the probe experiences greater energy loss, resulting in a steeper intensity gradient. This, in turn, induces an asymmetric self-phase modulation, which elevates the instantaneous frequency. It is notable that the laser in plasma exhibits opposite group velocity dispersion compared to traditional solid-state media. This unique property allows laser pulses to undergo dispersion compensation while broadening the spectrum, ultimately leading to self-compression. The 2D-PIC simulations demonstrate these phenomena, highlighting how period density-modulated plasma contributes to an asymmetric spectral distribution. The intricate interplay among self-phase modulation, group velocity, and backward Raman scattering results in the self-compressing of the laser pulse. Specifically, the pulses are compressed from their Fourier transform limit duration of 50 fs to a significantly reduced duration of 8 fs at plasma densities below 1/4 critical density, without the transverse self-focusing effects.

DOI: 10.1103/PhysRevE.109.065208

I. INTRODUCTION

Over the past several decades, the escalation of laser technologies has promoted the widespread exploration of intense few-cycle lasers for applications in particle acceleration [1], x-ray generation [2], high-order harmonic generation [3], and attosecond pulse radiation [3]. Despite advancements facilitated by chirped pulse amplification technology [4], which has enabled the development of petawatt (PW) lasers globally, constraints on pulse duration persist due to the bandwidth limitations of the gain medium and gain narrowing during the amplification. Typically, for Ti:sapphire-based laser systems, the pulse durations are commonly observed to fall within the range of 20 to 30 femtoseconds [5–7]. Even when employing optical parametric chirped pulse amplification (OPCPA) systems, which are renowned for the broader gain bandwidth, the output pulse duration is still close to 20 femtoseconds [8].

Post-compression techniques based on self-phase modulation (SPM) have emerged for effective methods for obtaining intense few-cycle pulses. Nevertheless, the implementation of methods such as solid thin plates [9], hollow-core fiber [10], or multipass cells (MPCs) [11] necessitates the chirped mirrors. This presents a challenge due to the damage threshold and the size limitations of chirped mirrors, particularly in achieving full energy dispersion compensation [12,13].

Plasmas known for their ability to withstand higher laser intensity than traditional optical components and anomalous dispersion properties have been extensively utilized in generating and manipulating ultrashort ultraintense lasers [14–18]. The potential of plasma-based techniques for self-compression of laser pulse has been both theoretically and experimentally demonstrated by various approaches, including the relativistic intensity pulse driving plasma waves [19,20], ionization-induced self-compression under weak relativistic mechanisms [21–24], and plasma amplification [25–28]. In these techniques, pulse compression relies on the nonlinearity arising from high intensity [29], high plasma density [30], or long interaction distance [31], where pulse intensities approach or exceed the relativistic threshold, and plasma lengths are typically in the order of millimeters (mm). However, the high nonlinearity may results in the bending of the wavefront, potentially leading to self-focusing or filamentation within longer plasma [29,30,32]. To mitigate the effects of filamentation, Shhorokhov *et al.* have employed a periodic plasma-vacuum structure with a plasma density spanning from 1/4 to near critical density to induce self-compression in weakly relativistic lasers [33].

To address these challenges, it is essential to extend self-compression to the realm of laser pulses with low intensity and plasma with low density. Such an extension could be of significant importance for the experimental realization of laser pulses with large energy and few-cycle durations.

In this Letter, we present two-dimensional (2D) particle-in-cell (PIC) simulations that demonstrate the self-compression

*Contact author: zhwang@iphy.ac.cn
†Contact author: zywei@iphy.ac.cn

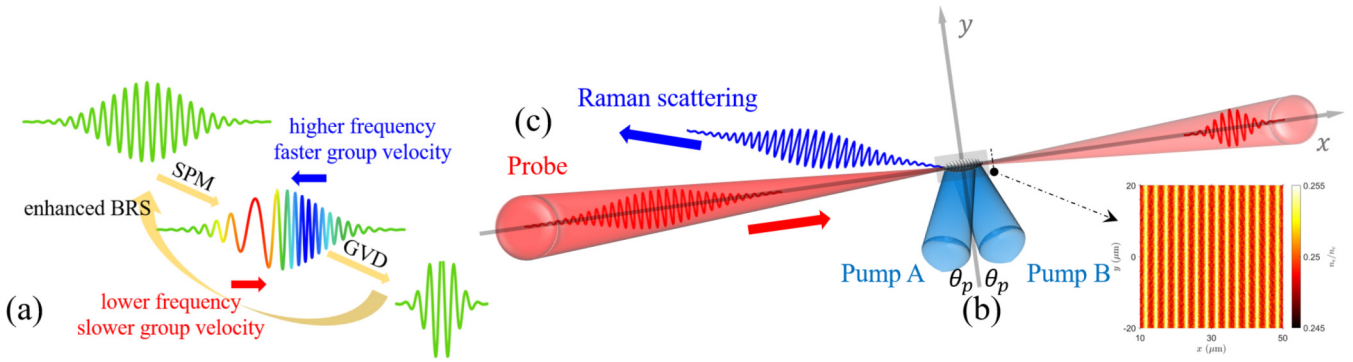

FIG. 1. Schematic of laser pulse self-compression aided by backward Raman scattering. (a) Self-compression method of laser pulse based on the combination of self-phase modulation, group velocity dispersion, and backward Raman scattering in plasma. (b) Two pump lasers cross the plasma along the y axis, and the overlapping part generates a periodic density-modulated plasma. (c) Within the picosecond persistence, a probe laser passes through the modulated plasma and is self-compressed to a few-cycle pulse.

of weakly relativistic laser pulses in a periodic density-modulated plasma below the 1/4 critical density, with the normalized vector potential a_0 approximately equal to 0.2. This corresponds to an intensity of approximately 10^{17} W/cm^2 for 800 nm light. The plasma, which serves as a compression medium with a one-dimensional index structure, is generated via the ponderomotive ion mechanism, a process that capitalizes on the interference patterns from two cross-propagating, low-intensity pump beams [17,34–37]. The simulations demonstrate that the trailing edge of the probe pulse experiences considerable energy loss, a consequence of Raman instability caused by the plasma with a density modulation of $\delta n_e = 2\%$ over picosecond. The sharpness of the pulse's trailing edge amplifies the change in the refractive index of plasma ($\partial n/\partial t$), leading to additional broadening and asymmetry in the spectrum. The synergy of asymmetric self-phase modulation (SPM), anomalous group velocity dispersion (GVD) in the plasma, and backward Raman scattering results in a pulse to self-compress from its Fourier transform limit duration of 50 fs to approximately 8 fs. Furthermore, the sinusoidal modulation structure in the density of plasma, combined with the lower intensity of the laser pulses, and a shorter interaction distance, effectively suppress the self-focusing effects of the laser pulse, resulting in an output pulse with high spatial mode quality.

II. THE MODEL OF LASER PULSES SELF-COMPRESSION IN PERIOD DENSITY-MODULATED PLASMA

The schematic of laser pulse self-compression aided by backward Raman scattering in period density-modulated plasma is depicted in Fig. 1. This figure illustrates how the laser pulse significantly self-compresses as shown in Fig. 1(a). This process is characterized by the higher frequency components at the leading of the pulse, which are induced by self-phase modulation (SPM), exhibiting relatively slower group velocities. In contrast, the lower frequency components at the trailing edge of the pulse advance with relatively fast group velocities, resulting in the self-compression of the laser pulse. Furthermore, periodic density-modulated plasma induces backward Raman scattering, which results in a steep gradient in the refractive index and further enhances SPM and GVD at the trailing edge of the probe pulse. The resultant broader spectrum and greater ability for dispersion compensation pave the way for further self-compression of laser pulses. Two pump laser beams with equal power and characterized by a wavelength $\lambda_0 = 800$ nm and a duration $\tau = 600$ fs initially cross the plasma along the y axis at a small angle $2\theta_0$ as illustrated in Fig. 1(b) [34,35]. The overlapping part of these beams produces an intensity distribution with a periodicity of $\Lambda = \lambda_0/2\sin\theta_0$. This periodic distribution leads to electrons experiencing varying ponderomotive forces at different spatial positions. Consequently, electrons continuously bunch within low-intensity regions, thereby forming a space-charge field [14]. This field exerts an influence on the ions, culminating in the formation of a one-dimensional density-modulated structure, as shown in the bottom right inset of Fig. 1. The modulation of the refractive index is produced in the x direction as the refractive index in the plasma varies with the plasma density. This relationship is defined by the expression $n = \sqrt{1 - \frac{n_e}{n_c}}$, where n_e is the electron density and n_c is the critical density. The periodic density-modulated plasmas generated by the ponderomotive ion mechanism [37] exhibit a persistence on the order of picoseconds. Within this timeframe, the probe, as it traverses the plasma along the x axis, can be significantly self-compressed, as shown in Fig. 1(c). The pulse self-compression is subject to variation based on the initial plasma density and the intensity of the probe.

In solution theory [29,38,39], the evolution of the laser pulse within the plasma is determined by the initial conditions of the laser pulse, namely its intensity and duration, as well as the density of the plasma. The interplay of these factors can result in various pulse duration behaviors, including broadening, compression, or oscillation around the soliton solution. Self-compression can typically be achieved with laser pulses of longer duration ($\tau > 30$ fs) [33]. We consider a linearly polarized laser pulse propagating along the x axis: $\mathbf{E}(t,z) = a(t,z)\cos(\Phi(t,z))\hat{\mathbf{y}}$. Here, $a(t,z)$ represents the pulse envelope, $\Phi(t,z) = \omega_0 t - z\omega_0 n/c$ is the phase, ω_0 is the angular

carrier frequency, n denotes the plasma refractive index, and c denotes the speed of light in vacuum. The instantaneous frequency of the laser pulse is defined as the time derivative of the phase [40,41]

$$\omega_t(t,z) = \frac{\partial \Phi}{\partial t} = \omega_0 - \frac{\omega_0}{c}\frac{\partial n(t,z)}{\partial t} z. \tag{1}$$

The formula above demonstrates the influence of the medium through which the laser pulse traverses on its instantaneous frequency. This interaction results in the generation of new spectral components and indicates spectrum broadening. For relativistic laser intensity, the refractive index experienced by the laser pulse when propagating through the plasma is given by [42,43] $n = \sqrt{1 - \frac{\omega_p^2}{\omega_0^2}\frac{1}{\gamma}}$. Here $\gamma = \sqrt{1+a^2}$ refers to the relativistic factor, dependent on the pulse intensity (a is the normalized vector potential), and ω_p is the resonance frequency corresponding to the plasma density. In the case of low density plasma, where $\omega_p^2 \ll \omega_0^2$, the equation can be simplified by denoting $\frac{\omega_p^2}{\omega_0^2}$ as N:

$$n \approx 1 - \frac{1}{2} N \frac{1}{\sqrt{1+a^2}}. \tag{2}$$

Substituting Eq. (2) into Eq. (1) allows the instantaneous frequency and the variation caused by self-phase modulation of high-intensity lasers in plasma to be obtained:

$$\omega_t(t,z) \approx \omega_0 - \omega_0 \frac{z}{c}\left(\frac{N}{2} a \frac{\partial a}{\partial t}\right), \quad \delta\omega = \omega_0 \frac{z}{c}\left(\frac{N}{2} a \frac{\partial a}{\partial t}\right). \tag{3}$$

The alteration of the laser pulse envelope results in the generation of new spectral components. The photon frequency shift caused by laser propagation in plasma is mainly determined by the normalized laser intensity a and the intensity change $\partial a/\partial t$. At the leading of the laser pulse, the change in the refractive index caused by the laser ($\partial n/\partial t > 0$) results in a downshift of the photon frequency. However, photons at the pulse trailing edge experience a frequency upshift as a result of the refractive index change characterized by a negative derivative ($\partial n/\partial t < 0$). In contrast, there is scarcely any frequency change in the center part of the pulse where the light intensity changes gradually.

The group velocity dispersion of laser pulses propagating through the medium can be expressed as $v_g = \frac{d\omega}{dk} = \frac{c}{n+\omega\frac{dn}{d\omega}}$. Applying this concept to a relativistic laser pulse propagating through a plasma, the group velocity dispersion can be calculated as

$$v_g = c\sqrt{1 - \frac{\omega_p^2}{\omega^2}\frac{1}{\gamma}} \approx c\sqrt{1 - \frac{N}{\left(1 - \frac{\delta\omega}{\omega_0}\frac{c}{z}\right)^2}}, \tag{4}$$

which is also determined by the instantaneous frequency variation. Here, γ is the relativistic factor, ω_p is the plasma frequency, N is a normalized plasma frequency parameter, $\delta\omega$ is the variation in the instantaneous frequency, ω_0 is the central angular frequency of the laser pulse, and z is the propagation distance within the plasma. Plasmas can provide more dispersion with the steeper pulse shapes, which results in a larger laser intensity gradient.

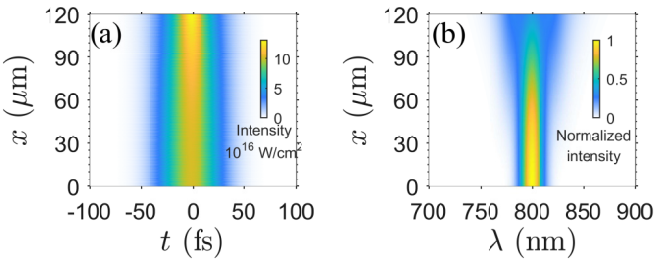

FIG. 2. Self-phase modulation in the plasma with constant density. (a) The pulse temporal shapes, and (b) the normalized spectrum distribution.

The combined effects of SPM and GVD can result in the self-compression of laser pulses during the propagation of a high-intensity laser in plasma. This is attributed to the anomalous group velocity dispersion described in Eq. (4), which dictates that photons experiencing a frequency downshift at the leading edge of the pulse will have a slower group velocity dispersion, whereas photons with a frequency upshift at the trailing edge of the pulse will display a faster group velocity dispersion. A Gaussian pulse with an initial pulse duration $\tau = 50$ fs and a normalized vector potential $a = 0.22$ propagates through a homogeneous plasma with a density of $0.25n_c$ and a plasma interaction length of 120 μm. Figures 2(a) and 2(b) illustrate the evolution of the pulse temporal shape and spectrum, respectively. These representations are derived from the numerical solution of the one-dimensional nonlinear Schrödinger equation [33], which in this context is simplified to include only the terms for SPM and GVD. The results suggest that the pulse can self-compress, reducing its duration from 50 fs to 35 fs with a compression factor of only 1.4.

To enhance the self-compression, it is proposed that the backward Raman scattering effect should be considered as a mechanism of energy consumption. For the laser-plasma interaction, the leading edge of the laser pulse induces the backward Raman scattering and growth of localized electron plasma waves (EPWs), and EPWs grow to saturation at the trailing edge of the laser pulse. This process causes the energy of the laser trailing to be seriously scattered, resulting in a steep pulse trailing edge and a large localized intensity gradient. The instantaneous frequency change caused by self-phase modulation and group velocity dispersion in plasma, closely related to the intensity gradient in Eqs. (1) and (2), also becomes larger. The expansion of the spectrum and greater ability for dispersion compensation are instrumental in driving further self-compression of laser pulses. Previous studies have demonstrated that for long laser pulses ($cT \ll \lambda_p$) and plasma densities above $1/4n_c$, the Raman instability is effectively suppressed and can be disregarded in the discussion [33]. However, in the periodic density-modulated plasma depicted in Fig. 1, where the plasma density is situated in a low-density region and the growth of SRS relies on density modulation [44], it is necessary to account for the Raman instability during the compression process. It is assumed that the plasma density fluctuation induced by the ponderomotive ion mechanism can be described by a sinusoidal modulation of the term $n_e(x) = n_{e0}[1 + \delta\sin(k_s x)]$, where n_{e0} represents the initial plasma electron density, $\delta = \Delta n/n_{e0}$ is the

amplitude of density modulation, and $k_s = 2\pi/\Lambda$ denotes the wave number of modulation. For stimulated Raman scattering within a density-modulated plasma, the wave number mismatch is represented by $\partial_x \Delta k$, where $\Delta k(x) = k_0 - k_1 - k_L(x)$ and $k_{0,1,L}$ correspond to the wave numbers of the incident laser, backward scattering signal, and plasma wave, respectively. In the case of sine modulation, $\omega_p^2 = \omega_p^2(x) = n_{e0}[1 + \delta \sin(k_s x)]e^2/m_e\epsilon_0$, so

$$\partial_x \Delta k = \kappa'' \cos(k_s x) \approx \frac{\omega_p^2(x=0)\delta k_s}{3v_{th}^2 k_L} \cos(k_s x). \quad (5)$$

Here, κ'' is the coefficient of wave number detuning, where $v_{th} = \sqrt{k_B T_e/m_e}$ is the thermal motion rate of the electron, and k_B and T_e are the Boltzmann constant and plasma temperature, respectively. Picard's [45] theory demonstrates that the time growth rate of SRS is related to the wave number k_s and amplitude δ of the density modulation, and absolute instability can occur when sinusoidal density modulation is present in the system. As detailed in Ref. [46], employing a plasma with long-wavelength small-amplitude modulation characterized by $k_s = 0.03k_0$, $\delta \approx 0.02$ can induce the absolute SRS, resulting in a marked improvement of the backward reflectance of the incident laser pulse. The key to achieving this lies in the judicious selection of the appropriate wave number k_s and amplitude δ, which leads to the continuous consumption of the trailing edge of the pulse. Hence, the interaction proposed between a laser and a periodic density-modulated plasma can give rise to the significant backward Raman scattering of laser pulses with lower light intensity in the low-density plasma region. The combination of self-phase modulation, group velocity dispersion, and backward Raman scattering can lead to significant self-compression of laser pulses.

III. PIC SIMULATION RESULTS

To fully simulate the laser pulse self-compression process in a sinusoidal modulated plasma, two-dimensional simulations are performed using the fully relativistic PIC simulation code EPOCH [47]. The size of the simulation box is 240 μm(x) × 120 μm(y), with grid cells of 9600 × 600 and ten particles per cell. A vacuum region of 60 μm is allocated at each extremity of the x axis. The fully ionized hydrogen plasma is crossed by two pump beams ($\lambda_0 = 800$ nm, $I = 2 \times 10^{15}$ W/cm^2) with the pulse duration of 600 fs along the y axis at a small angle, which generates the periodic density-modulated plasma. The periodic modulation, driven by the ponderomotive force, is sustained on picosecond timescales. The probe pulse is introduced into the simulation after a delay time of 2 ps. The probe pulse propagates along the x axis with a linear polarization and a wavelength of $\lambda_1 = 800$ nm. It is initialized with a pulse duration of $\tau = 50$ fs and a spot size of 40μm full width at half maximum (FWHM). The peak intensity of the probe pulse is $I = 1 \times 10^{17}$ W/cm^2 ($a \approx 0.22$), denoted by a normalized vector potential $a \approx 0.22$, which is chosen to ensure a sufficient nonlinear response while avoiding self-focusing and nonlinear plasma waves that could arise from high relativistic nonlinearity. The initial electron temperature is $T_e = 10$ eV and the ion temperature is $T_e = 1$ eV.

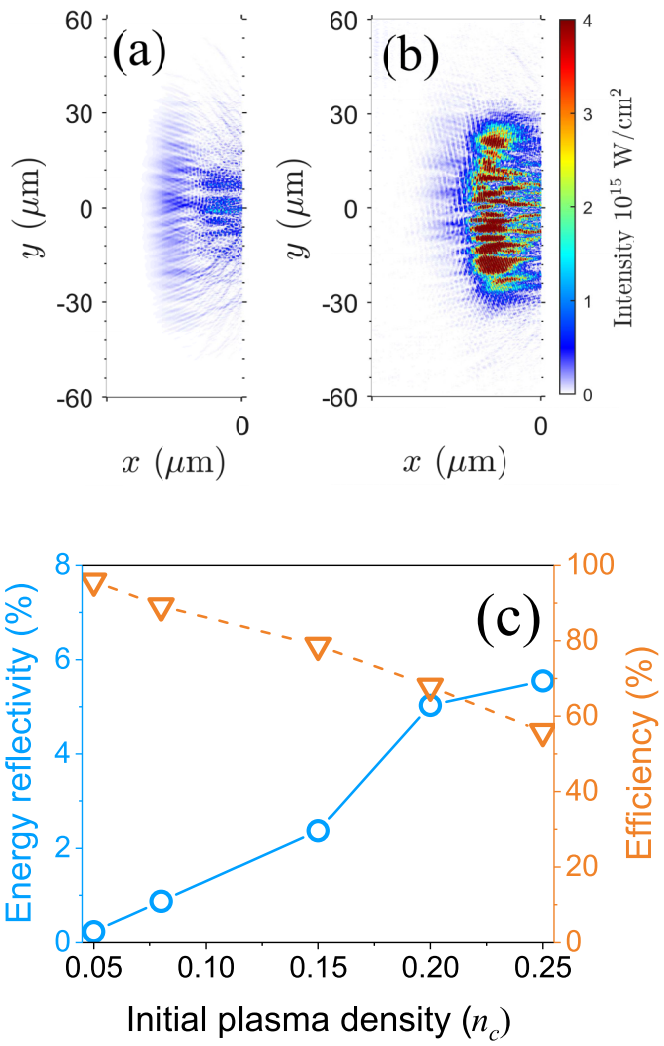

FIG. 3. The enhancement of backward Raman scattering in the period density modulated plasma. The intensity of backward Raman scattering signals at $t = 200$ fs in the constant plasma with $n_e = 0.25n_c$ (a) and in the period density modulated plasma with $n_e = 0.25n_c$ (b). (c) Energy reflectivity (E_R/E_{In}) of the left vacuum region at t=200 fs and the pulse self-compression efficiency ($E_{\text{Out}}/E_{\text{In}}$) in the period density modulated plasmas with different initial plasma density.

Figure 1 presents a schematic of two pump beams with equal intensity at an angle of 8.1° along the y axis through a fully ionized hydrogen plasma. The plasma has a density varying from $0.05n_c$ to $0.25n_c$, where n_c is the critical density corresponding to a wavelength $\lambda = 800$ nm. The ponderomotive ion force drives the electrons and ions away from the high intensity region of spatial interference, resulting in a sinusoidal density modulation. This modulation can be characterized by its long wavelength and small amplitude. The modulation period, denoted by Λ, is approximately 2.84 μm, which corresponds to a wave number of $k_s \approx 0.28k_0$, and the modulation amplitude $\delta \approx 0.02$. The combinations of parameters, such k_s and δ have been demonstrated to increase the reflectivity of SRS [46]. Figures 3(a) and 3(b) show the intensity distribution of the scattering signal in the left vacuum

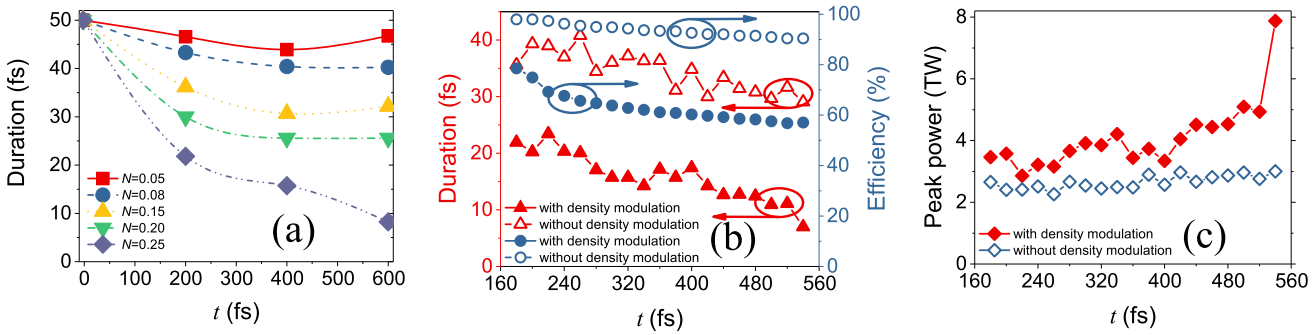

FIG. 4. Self-compression of laser pulses in the period density modulated plasma. (a) Dependence of pulse duration on the plasma density ($N = \omega_p^2/\omega_0^2$). (b) Effect of the period density modulated structure on the duration (the solid red triangles and the hollow red triangles) and self-compression efficiency (the solid blue dots and the hollow blue dots) of the probe pulse. (c) Evolution of the pulse peak power with (the solid red rhombus) or without (the hollow blue rhombus) the period density modulated plasma.

region at the instance when the probe pulse enters the plasma completely ($t = 200$ fs) with a constant density $n_e = 0.25n_c$ and the periodic modulation density mentioned above, respectively. The comparison of the two scattering intensities indicates that density modulation significantly enhances backward scattering, and the spectral analysis confirms that the scattering signals are derived from the Raman scattering of the probe pulse. Figure 3(c) illustrates the influence of the initial plasma density n_e on the energy reflectivity $E_R/E_{\rm In}$ within the left vacuum region at t=200 fs, as well as on the pulse self-compression efficiency $E_{\rm Out}/E_{\rm In}$. The inhomogeneous growth rate of BRS $\gamma_{\rm inh}$ is intimately connected to the wave number mismatch coefficient κ'' through the relation $\gamma_{\rm inh} \equiv |\kappa''|^{1/3}$, so as expressed in Eq. (5), the inhomogeneous growth rate of BRS increases with $\omega_p^2(x = 0)$. Consequently, this correlation leads to an increase in energy reflectivity and a decrease in the self-compression efficiency of the probe pulse with the increase of the initial plasma density. Within the plasma, Raman scattering transfers energy through the excitation of EPWs, which are generated by the beat of the pump and scattering light. As previously discussed in Sec. II, this results in a relatively greater energy loss at the trailing edge of the probe, yet simultaneously improves the local intensity gradient, induces more spectrum broadening brought by SPM, and ultimately leads to further self-compression with more significant GVD.

Figure 4(a) shows the impact of varying initial plasma densities on the duration of the probe pulse in a period density-modulated plasma. The results indicate that higher plasma densities lead to shorter probe pulse durations due to the energy loss at the trailing edge of the pulse and the enhanced self-compression of the pulse, which is a consequence of the combination of SPM and GVD. Additionally, the influence of the period density modulation on both the pulse duration and pulse self-compression efficiency $E/E_{\rm In}$ of the probe is investigated. The detailed results are presented in Fig. 4(b) for the plasma with density $n_e = 0.25n_c$. The interaction of an intense laser pulse with the constant density plasma causes a combination of SPM and GVD, resulting in a slight compression of the pulse duration from 50 fs to approximately 31 fs as represented by the hollow red triangles. This duration is slightly shorter than that derived from the one-dimensional nonlinear Schrödinger equation, which considers only SPM and GVD terms in Fig. 2(a). This discrepancy indicates that the laser energy consumption from BRS contributes less to pulse self-compression. Furthermore, it is observed that the pulse energy is consumed smoothly, with only a 10% loss ultimately occurring, as indicated by the hollow blue dots. In contrast, the periodic density-modulated plasma induces a significantly greater self-compression of the laser pulse, reducing its duration by a factor of over six, from 50 fs to around 8 fs, as depicted by the solid red triangles. As predicted by the theoretical analysis in Sec. II, backward Raman scattering is associated with increased energy loss in the period density-modulated plasma. Initially, the laser energy with a longer pulse duration is severely consumed by BRS, but as the pulse duration of the probe decreases, the energy loss gradually decreases, and only approximately 55% of the energy is retained at the end, as shown by the solid blue dots. The purpose of pulse compression is to obtain a shorter laser pulse and to increase the laser peak power, so we show the evolution of the laser peak power in Fig. 4(c). Within a plasma of constant density, represented by the hollow blue rhombus, the peak power exhibits a gradual increase over time, while a more significant improvement in peak power is observed within the periodic density-modulated plasma, as depicted by the solid red rhombus. It is a well-established principle in laser physics that the laser peak power is described by the pulse energy E and pulse duration τ, expressed by $P_{peak} = E/\tau$. The energy consumed by period modulation is indeed instrumental in compressing the pulse, but this does not inherently lead to an enhancement of peak power. Nevertheless, as depicted in Fig. 5(a), the sharper intensity gradient generated by BRS at the trailing edge of the pulse induces a localized intensification of SPM and GVD. This observation suggests that the better self-compression observed in plasma with periodic density modulation is not solely a consequence of laser energy depletion. Instead, it is the combination of SPM, anomalous GVD, and BRS that improves the self-compression within the modulated plasma.

Figures 5(a) and 5(b) present the spatial intensity distributions at the initial, intermediate (within the plasma), and final stages of the interaction between the probe pulse and two distinct plasma structures: one with periodic density modulation and another with a constant density at $n_e = 0.25n_c$. Each temporal snapshot is captured at an interval of 180 fs. In the spatial domain, the phenomenon of pulse self-compression

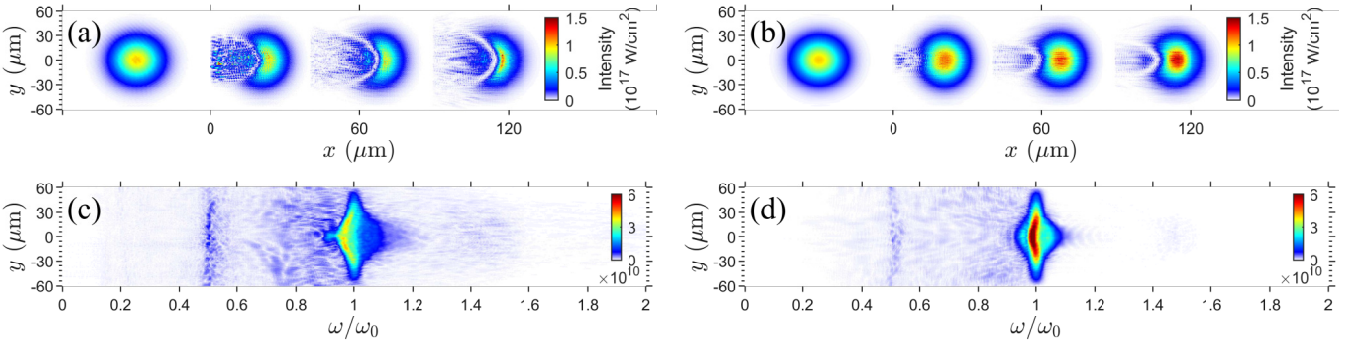

FIG. 5. Comparison of pulse evolution for two different plasma structures. (a) Pulse evolution in the period density modulated plasma with $n_e = 0.25n_c$. (b) Pulse evolution in the constant density plasma with $n_e = 0.25n_c$. (c) The spectrum of the output pulse at different spatial positions (y) in the period density modulated plasma. (d) The spectrum of the output pulse at different spatial positions (y) in the constant density plasma.

is observed for both cases. Furthermore, a post-pulse is observed in the spatial distribution, which can be attributed to the combination of the π-pulse structure characteristic of the backward Raman scattering and the pulse splitting that occurs during the compression process. It is noteworthy that the entire interaction is accompanied by a significant backward (side) scattering signal. Figures 5(c) and 5(d) illustrate the spectrum of various spatial positions (y) at the final moment of Figures 5(a) and 5(b). The evolution of the pulse temporal shape observed in 5(a) and the further spectral broadening evident in 5(c), indicate that periodic density modulation significantly enhances the self-compression of the laser pulse. The spectrum's spindlelike shape is attributable to the Gaussian distribution of the pulse's spatial intensity, which leads to intensity-dependent spectral broadening. Consequently, the spectrum's maximum value, located along the axis at y=0, gradually decreases toward the periphery. Furthermore, periodic density modulation enhances backward Raman scattering and increases the intensity gradient at the pulse trailing, which results in asymmetric self-phase modulation and reduces the frequency upshift of photons at the trailing edge of the probe pulse. The frequency matching relation for a laser within a plasma is defined by $\omega_0^2 = \omega^2 + \omega_p^2$, where ω_0 signifies the laser frequency, ω represents the scattered frequency, and ω_p denotes the plasma frequency. This relation indicates that the frequency of the backward scattering signal $ck_{SRS}/\omega_0 \approx 0.5$. Furthermore, the difference in spectral intensity between Figs. 5(c) and 5(d) around $\omega \approx 0.5\omega_0$ provides robust evidence that periodic density modulation enhances backward Raman scattering.

In conclusion, we have presented and simulated the self-compression of laser pulses in the plasma below 1/4 of the critical density. The observed phenomena are rooted in the interplay of self-phase modulation (SPM), group velocity dispersion (GVD), and backward Raman scattering (BRS). The simulation results suggest that the increased backward Raman scattering of the probe pulse induces the modification in the pulse intensity gradient at the trailing edge within the periodic density-modulated plasma. The plasma is characterized by a long-wavelength, low-amplitude period modulation, and picosecond persistence, leading to a localized alteration of the instantaneous spectrum based on the intensity gradient within the pulse. The compensation of group velocity dispersion enables the self-compression from 50 fs to 8 fs. The trajectory of the laser's peak power throughout the simulation indicates that the better self-compression observed in the periodic density-modulated plasma is induced by the combination of SPM, anomalous GVD, and BRS instead of laser depletion. The spectral domain analysis has unveiled an asymmetry in the spectral intensity distribution and self-phase modulation. Our research demonstrates that by manipulating the structure of low-density plasma, it is possible to achieve self-compression of laser pulses with lower intensities. This development paves the way for advancing laser pulses into a realm of few-cycle durations and hundred millijoule energy, or even joule energy. Such an achievement holds significant promise for the generation of high-energy attosecond pulses, expanding the horizons of laser-plasma interactions and their applications.

ACKNOWLEDGMENTS

All numerical calculations in this paper were done at Beijing Super Cloud Computing. This work was supported by the CAS Project for Young Scientists in Basic Research (Grant No. YSBR-065), the National Natural Science Foundation of China (Grants No. 62335004 and No. 12304385), the National Key R&D Program of China (2023YFA1608501), and the Synergetic Extreme Condition User Facility (SECUF).

[1] E. Esarey, C. B. Schroeder, and W. P. Leemans, Physics of laser-driven plasma-based electron accelerators, Rev. Mod. Phys. **81**, 1229 (2009).

[2] S. Kiselev, A. Pukhov, and I. Kostyukov, X-ray generation in strongly nonlinear plasma waves, Phys. Rev. Lett. **93**, 135004 (2004).

[3] F. Krausz and M. Ivanov, Attosecond physics, Rev. Mod. Phys. **81**, 163 (2009).

[4] D. Strickland and G. Mourou, Compression of amplified chirped optical pulses, Opt. Commun. **56**, 219 (1985).

[5] Z.-H. Wang, C. Liu, Z.-W. Shen, Q. Zhang, H. Teng, and Z.-Y. Wei, High-contrast 1.16 PW Ti:sapphire laser system

combined with a doubled chirped-pulse amplification scheme and a femtosecond optical-parametric amplifier, Opt. Lett. **36**, 3194 (2011).

[6] W. Li, Z. Gan, L. Yu, C. Wang, Y. Liu, Z. Guo, L. Xu, M. Xu, Y. Hang, Y. Xu, J. Wang, P. Huang, H. Cao, B. Yao, X. Zhang, L. Chen, Y. Tang, S. Li, X. Liu, S. Li *et al.*, 339 J high-energy Ti:sapphire chirped-pulse amplifier for 10 PW laser facility, Opt. Lett. **43**, 5681 (2018).

[7] C. Radier, O. Chalus, M. Charbonneau, S. Thambirajah, G. Deschamps, S. David, J. Barbe, E. Etter, G. Matras, S. Ricaud, *et al.*, 10 PW peak power femtosecond laser pulses at ELI-NP, High Power Laser Science and Engineering **10**, e21 (2022).

[8] X. Zeng, K. Zhou, Y. Zuo, Q. Zhu, J. Su, X. Wang, X. Wang, X. Huang, X. Jiang, D. Jiang, Y. Guo, N. Xie, S. Zhou, Z. Wu, J. Mu, H. Peng, and F. Jing, Multi-petawatt laser facility fully based on optical parametric chirped-pulse amplification, Opt. Lett. **42**, 2014 (2017).

[9] C.-H. Lu, Y.-J. Tsou, H.-Y. Chen, B.-H. Chen, Y.-C. Cheng, S.-D. Yang, M.-C. Chen, C.-C. Hsu, and A. H. Kung, Generation of intense supercontinuum in condensed media, Optica **1**, 400 (2014).

[10] T. Nagy, M. Kretschmar, M. J. J. Vrakking, and A. Rouzée, Generation of above-terawatt 1.5-cycle visible pulses at 1 khz by post-compression in a hollow fiber, Opt. Lett. **45**, 3313 (2020).

[11] S. Rajhans, E. Escoto, N. Khodakovskiy, P. K. Velpula, B. Farace, U. Grosse-Wortmann, R. J. Shalloo, C. L. Arnold, K. Põder, J. Osterhoff, W. P. Leemans, I. Hartl, and C. M. Heyl, Post-compression of multi-millijoule picosecond pulses to few-cycles approaching the terawatt regime, Opt. Lett. **48**, 4753 (2023).

[12] J. I. Kim, Y. G. Kim, J. M. Yang, J. W. Yoon, J. H. Sung, S. K. Lee, and C. H. Nam, Sub-10 fs pulse generation by post-compression for peak-power enhancement of a 100-tw ti:sapphire laser, Opt. Express **30**, 8734 (2022).

[13] P.-G. Bleotu, J. Wheeler, S. Y. Mironov, V. Ginzburg, M. Masruri, A. Naziru, R. Secareanu, D. Ursescu, F. Perez, J. De Sousa *et al.*, Post-compression of high-energy, sub-picosecond laser pulses, High Power Laser Science and Engineering **11**, e30 (2023).

[14] Z. Nie, C.-H. Pai, J. Hua, C. Zhang, Y. Wu, Y. Wan, F. Li, J. Zhang, Z. Cheng, Q. Su *et al.*, Relativistic single-cycle tunable infrared pulses generated from a tailored plasma density structure, Nat. Photonics **12**, 489 (2018).

[15] F. Amiranoff, C. Riconda, M. Chiaramello, L. Lancia, J. R. Marquès, and S. Weber, The role of the global phase in the spatio-temporal evolution of strong-coupling Brillouin scattering, Phys. Plasmas **25**, 013114 (2018).

[16] H. Peng, J.-R. Marquès, L. Lancia, F. Amiranoff, R. L. Berger, S. Weber, and C. Riconda, Plasma optics in the context of high intensity lasers, Matter Radiat. Extremes **4**, 065401 (2019).

[17] M. R. Edwards and P. Michel, Plasma transmission gratings for compression of high-intensity laser pulses, Phys. Rev. Appl. **18**, 024026 (2022).

[18] M. R. Edwards, V. R. Munirov, A. Singh, N. M. Fasano, E. Kur, N. Lemos, J. M. Mikhailova, J. S. Wurtele, and P. Michel, Holographic Plasma Lenses, Phys. Rev. Lett. **128**, 065003 (2022).

[19] J. Schreiber, C. Bellei, S. P. D. Mangles, C. Kamperidis, S. Kneip, S. R. Nagel, C. A. J. Palmer, P. P. Rajeev, M. J. V. Streeter, and Z. Najmudin, Complete temporal characterization of asymmetric pulse compression in a laser wakefield, Phys. Rev. Lett. **105**, 235003 (2010).

[20] X.-L. Zhu, S.-M. Weng, M. Chen, Z.-M. Sheng, and J. Zhang, Efficient generation of relativistic near-single-cycle mid-infrared pulses in plasmas, Light Sci. Appl. **9**, 46 (2020).

[21] W. M. Wood, C. W. Siders, and M. C. Downer, Measurement of femtosecond ionization dynamics of atmospheric density gases by spectral blueshifting, Phys. Rev. Lett. **67**, 3523 (1991).

[22] N. L. Wagner, E. A. Gibson, T. Popmintchev, I. P. Christov, M. M. Murnane, and H. C. Kapteyn, Self-compression of ultrashort pulses through ionization-induced spatiotemporal reshaping, Phys. Rev. Lett. **93**, 173902 (2004).

[23] S. A. Skobelev, A. V. Kim, and O. Willi, Generation of high-energy few-cycle laser pulses by using the ionization-induced self-compression effect, Phys. Rev. Lett. **108**, 123904 (2012).

[24] Z.-H. He, J. A. Nees, B. Hou, K. Krushelnick, and A. G. R. Thomas, Ionization-induced self-compression of tightly focused femtosecond laser pulses, Phys. Rev. Lett. **113**, 263904 (2014).

[25] R. Trines, F. Fiuza, R. Bingham, R. Fonseca, L. Silva, R. Cairns, and P. Norreys, Simulations of efficient raman amplification into the multipetawatt regime, Nat. Phys. **7**, 87 (2011).

[26] J. Ren, W. Cheng, S. Li, and S. Suckewer, A new method for generating ultraintense and ultrashort laser pulses, Nat. Phys. **3**, 732 (2007).

[27] H. Peng, Z. H. Wu, Y. L. Zuo, Z. M. Zhang, K. N. Zhou, and J. Q. Su, Single laser pulse compression via strongly coupled stimulated Brillouin scattering in plasma, Phys. Plasmas **23**, 073516 (2016).

[28] J. Li, X. Wang, Z. Wang, X. Zhang, J. Li, and Z. Wei, The effect of scattering instability induced by high intensity seed on backward Raman amplification, Appl. Phys. Lett. **123**, 171105 (2023).

[29] M. Lontano and I. G. Murusidze, Dynamics of space-time self-focusing of a femtosecond relativistic laser pulse in an underdense plasma, Opt. Express **11**, 248 (2003).

[30] B. Bokaei and A. R. Niknam, Weakly relativistic and ponderomotive effects on self-focusing and self-compression of laser pulses in near critical plasmas, Phys. Plasmas **21**, 103107 (2014).

[31] D. F. Gordon, B. Hafizi, R. F. Hubbard, J. R. Peñano, P. Sprangle, and A. Ting, Asymmetric self-phase modulation and compression of short laser pulses in plasma channels, Phys. Rev. Lett. **90**, 215001 (2003).

[32] C. Ren, B. J. Duda, R. G. Hemker, W. B. Mori, T. Katsouleas, T. M. Antonsen, and P. Mora, Compressing and focusing a short laser pulse by a thin plasma lens, Phys. Rev. E **63**, 026411 (2001).

[33] O. Shorokhov, A. Pukhov, and I. Kostyukov, Self-compression of laser pulses in plasma, Phys. Rev. Lett. **91**, 265002 (2003).

[34] H. Peng, C. Riconda, M. Grech, J.-Q. Su, and S. Weber, Nonlinear dynamics of laser-generated ion-plasma gratings: A unified description, Phys. Rev. E **100**, 061201(R) (2019).

[35] H. Peng, C. Riconda, M. Grech, C. Zhou, and S. Weber, Dynamical aspects of plasma gratings driven by a static ponderomotive potential, Plasma Phys. Controlled Fusion **62**, 115015 (2020).

[36] Z.-M. Sheng, J. Zhang, and D. Umstadter, Plasma density gratings induced by intersecting laser pulses in underdense plasmas, Appl. Phys. B **77**, 673 (2003).

[37] G. Lehmann and K. H. Spatschek, Transient plasma photonic crystals for high-power lasers, Phys. Rev. Lett. **116**, 225002 (2016).

[38] J. I. Gersten and N. Tzoar, Propagation of localized electromagnetic pulses in plasmas, Phys. Rev. Lett. **35**, 934 (1975).

[39] P. K. Kaw, A. Sen, and T. Katsouleas, Nonlinear 1d laser pulse solitons in a plasma, Phys. Rev. Lett. **68**, 3172 (1992).

[40] L. Mandel, Interpretation of Instantaneous Frequencies, Am. J. Phys. **42**, 840 (1974).

[41] T. Nagy, P. Simon, and L. Veisz, High-energy few-cycle pulses: Post-compression techniques, Adv. Phys.: X **6**, 1845795 (2021).

[42] P. Sprangle, E. Esarey, and A. Ting, Nonlinear theory of intense laser-plasma interactions, Phys. Rev. Lett. **64**, 2011 (1990).

[43] P. Sprangle, E. Esarey, and A. Ting, Nonlinear interaction of intense laser pulses in plasmas, Phys. Rev. A **41**, 4463 (1990).

[44] J. Li, R. Yan, and C. Ren, Density modulation-induced absolute laser-plasma-instabilities: Simulations and theory, Phys. Plasmas **24**, 052705 (2017).

[45] G. Picard and T. W. Johnston, Decay instabilities for inhomogeneous plasmas: WKB analysis and absolute instability, Phys. Fluids **28**, 859 (1985).

[46] Y. Chen, C. Zheng, Z. Liu, L. Cao, Q. Feng, Y. Chen, Z. Huang, and C. Xiao, Influences of sinusoidal density modulation on stimulated raman scattering in inhomogeneous plasmas, Plasma Phys. Controlled Fusion **63**, 055004 (2021).

[47] T. Arber, K. Bennett, C. Brady, A. Lawrence-Douglas, M. Ramsay, N. Sircombe, P. Gillies, R. Evans, H. Schmitz, A. Bell *et al.*, Plasma Phys. Controlled Fusion **57**, 113001 (2015).